Application of a Parallel Genetic Algorithm to the Global Optimization of Gas-Phase and Supported Gold-Iridium Sub-Nanoalloys

Davis, Jack; Horswell, Sarah L.; Johnston, Roy

[Link to publication on Research at Birmingham portal](#)

The Application of a Parallel Genetic Algorithm to the Global Optimisation of Gas-Phase and Supported Gold-Iridium Sub-Nanoalloys

Jack B. A. Davis, Sarah L. Horswell, and Roy L. Johnston[*]

School of Chemistry, University of Birmingham

E-mail: r.l.johnston@bham.ac.uk

Abstract

The direct density functional theory global optimisation of MgO(100)-supported AuIr sub-nanoalloys is performed using the Birmingham Parallel Genetic Algorithm (BPGA). The BPGA is a pool genetic algorithm for the structural characterisation of nanoalloys. The parallel pool methodology utilised within the BPGA allows the code to characterise the structures of $N = 4 - 6$ Au_nIr_{N-n} clusters in the presence of the MgO(100) surface. The use of density functional theory allows the code to capture quantum size effects in the system which determine their structures. The searches reveal significant differences in structure and chemical ordering between the surface-supported and gas-phase global minimum structures.

Introduction

Nanoalloys (NAs) are a class of nanomaterial composed of multiple metallic elements. The combination of metals results in properties which are not only dependent on the size and shape of the cluster but on the composition and ordering of elements.[1] NAs have potential optical, magnetic and catalytic applications.[2]

AuIr NAs have been investigated previously both theoretically and experimentally,[3–6] particularity for CO oxidation catalysis. The activity of monometallic Au CO oxidation catalysts was found to decrease over time, either because of sintering or poisoning.[7] The addition of Ir to the catalyst has been shown to prevent sintering and improve the overall catalytic activity of the system through the formation of nanoalloy particles.[3,5] In the studies of both the mono- and bimetallic Au systems, the support was shown to play an important role in the activity of the catalyst.[8,9]

The structural characterisation of NAs is a vital first step toward rationalising their catalytic properties. In the present study the structures of $N = 4 - 6$ Au_nIr_{N-n} NAs are characterised using direct DFT global optimisation. This is performed both in the gas-phase and in the presence of an MgO(100) slab to better understand the effect of a surface on the

structures of AuIr NAs. The use of direct DFT global optimisation is necessary to reveal any quantum size effects, commonly seen for Au and Ir, in the NA structures.[10]

Both the gas-phase and MgO(100)-supported global optimisations of the AuIr clusters are performed using the Birmingham Parallel Genetic Algorithm (BPGA).[11] The BPGA is a pool-based genetic algorithm, capable of performing multiple DFT calculations in parallel.[12] This parallelism is of particular importance for the surface-supported calculations. While numerous methods for the direct DFT global optimisation of surface-supported clusters have been developed,[13,14] the inclusion of a surface slab within a local minimisation increases the cost of the underlying DFT calculations and therefore greatly increases the overall cost of the global optimisation.

Methodology

DFT

Gamma-point, spin-polarised DFT calculations were performed with VASP.[15–19] Projected-augmented wave (PAW) pseudopotentials were used with the PBE exchange correlation functional.[20,21] A plane-wave basis set with a cut-off of 400 eV was used. Methfessel-Paxton smearing, with a sigma value of 0.01 eV, was utilised to improve SCF convergence.[22]

BPGA

The BPGA is an open-source genetic algorithm for the direct DFT global optimisation of nanoalloys.[23] The program utilises a pool methodology which allows the evaluation of multiple potential cluster geometries in parallel.[12,24] Calculations are performed in parallel with between 2 and 4 instances of the BPGA operating on shared pools, depending on the size of the cluster. Depending on access to computational resources, the number of instances could be far larger.

An initial pool of 10 random structures is generated and evaluated by local minimisation

within VASP. These initial structures are prepared so that no two atoms are so close as to be non-physical. Once the initial pool has been minimised, crossover and mutation operations are carried out. For crossover, pairs of clusters are selected from the pool through tournament selection. Offspring are then produced through single-point, weighted crossover, carried out according to the Deaven and Ho cut and splice method.[25] The mutation rate is set to 10% of the pool size.

For the supported clusters the local minimisation of the cluster geometry is performed in the presence of an MgO(100) slab, which is not relaxed during the calculation due to the high computational cost of doing so. The slab unit cell used in the present study is 6×6×2 atoms with a 14.7 Å vacuum spacing, to ensure there is no interaction between the cluster and the periodic cell. The use of two layers of MgO(100) has previously been shown to be capable of replicating the behaviour of the surface and its effect on the properties of a cluster.[26–29] The height of the cluster is fixed so that the lowest lying atom is 1.5 Å above the surface, as is shown in figure 1.
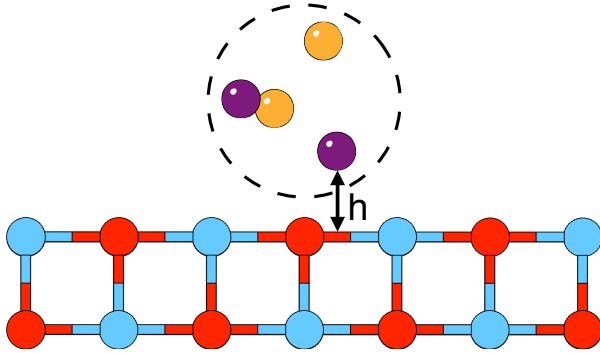
Figure 1: An initial random geometry is generated and placed at a fixed height, $h = 1.5$ Å, above the MgO(100) slab.

The mutation operator for the surface-supported clusters is a random rotation of the cluster with respect to the fixed slab. For the gas-phase clusters, the mutation operators are a random perturbation (up to a 1 Å displacement of 20% of the cluster atoms) for monometallic clusters and a homotop-swap for bimetallic clusters.

Crossover and mutation operations are performed until the highest and lowest energies

of the pool differ by no more than 10^{-3} eV. Due to the high computational cost, only one run is carried out per composition.

Energetics

The binding energies, E_b, were calculated using the following expression

$$E_b = \frac{E_{Au_n Ir_m} - (nE_{Au} + mE_{Ir})}{N} \tag{1}$$

where $E_{Au_n Ir_m}$ is the total energy of cluster $Au_n Ir_m$, E_{Au} and E_{Ir} are the energies of single, spin-polarised Au and Ir atoms and N is the total number of atoms ($N = n + m$).

The excess energies, Δ,[30] of the clusters was calculated using

$$\Delta = E_{Au_n Ir_m} - n \left(\frac{E_{Au_N}}{N} \right) - m \left(\frac{E_{Ir_N}}{N} \right) \tag{2}$$

where E_{Au_N} and E_{Ir_N} are the energies of the monometallic Au and Ir clusters with the same total number of atoms as $Au_n Ir_m$.

The adsorption energies E_{ads} of the surface -supported global minima were calculated as follows

$$E_{ads} = E_{slab + Au_n Ir_m} - (E_{slab} + E_{Au_n Ir_m}) \tag{3}$$

where E_{slab} is the energy of the MgO(100) slab and $E_{Au_n Ir_m}$ is the energy of the $Au_n Ir_m$ cluster, locally minimised in the gas-phase.

Results

The putative global minimum structures of the gas-phase $N = 4 - 6$ $Au_n Ir_{N-n}$ clusters are shown in figures 2, 3 and 4. Global minimum structures for the MgO(100)-supported $N = 4 - 6$ $Au_n Ir_{N-n}$ clusters are shown in figures 5, 6 and 7.

Table 1: Binding energies E_b (gas-phase only), adsorption energies E_{ads} (surface-supported only), excess energies Δ and spin-multiplicities $2S+1$ for the $N = 4-6$ Au_nIr_{N-n} clusters.

	Gas-Phase			Surface-Supported		
	E_b / eV	Δ / eV	$2S+1$	E_{ads} / eV	Δ / eV	$2S+1$
Au_4	-1.546	0	1	-1.951	0	1
Au_3Ir	-1.840	0.948	3	-2.342	0.890	3
Au_2Ir_2	-2.397	0.845	5	-3.251	0.332	3
$AuIr_3$	-2.928	0.843	5	-3.434	0.459	1
Ir_4	-3.670	0	9	-2.933	0	3
Au_5	-1.692	0	2	-1.973	0	2
Au_4Ir	-1.975	0.784	4	-2.341	0.317	2
Au_3Ir_2	-2.458	0.565	4	-2.963	0.132	2
Au_2Ir_3	-2.892	0.593	6	-2.784	0.371	4
$AuIr_4$	-3.478	-0.137	4	-3.083	-0.307	2
Ir_5	-3.890	0	8	-3.325	0	4
Au_6	-1.929	0	1	-1.592	0	1
Au_5Ir	-2.117	1.113	3	-2.465	1.356	1
Au_4Ir_2	-2.500	1.060	5	-3.621	0.830	3
Au_3Ir_3	-2.913	0.829	7	-3.559	0.574	1
Au_2Ir_4	-3.382	0.255	7	-3.211	0.847	3
$AuIr_5$	-3.730	0.415	7	-3.043	1.083	5
Ir_6	-4.173	0	5	-3.494	0	5

Global minima for the gas-phase and supported Au_nIr_{4-n} clusters are all found to be planar. The surface-supported global minimum structures are all found to be normal to the plane of the surface as a result of the 'metal-on-top effect' commonly seen in such subnanometre size clusters.[31] Ir_4 is found to be a square, as seen in previous studies of gas-phase Ir clusters,[32] and Au_4 is found to favour a rhombus structure. Differences between the gas-phase and adsorbed clusters are subtle. On the surface the structure of Au_4 is elongated so that two Au atoms can bond to two O atoms, increasing the Au-Au distance from 2.68 Å to 3.76 Å. The adsorbed structure of Ir_4 is the same as the gas-phase structure, with the square standing upright and bound to two O atoms.

All surface-supported bimetallic structures favour the stronger Ir-O interactions over Au-O. The structures of Au_3Ir, Au_2Ir_2 and $AuIr_3$ all differ from the gas-phase structures. The structures of Au_3Ir and Au_2Ir_2 are both Y-shaped in the gas-phase. On the surface the preferred structure is a rhombus, with Au_2Ir_2 having an elongated Au-Au bond. The gas-phase structure of $AuIr_3$ is a distorted rhombus. On the surface, the three Ir atoms form a linear chain with the Au atom bridging an Ir-Ir bond. In doing so $AuIr_3$ is able to maximise the number of Ir-O interactions.

The structure of the surface-supported Au_5 is similar to that of Au_4, with the structure again having an elongated Au-Au bond so as to bond across two O atoms. The structure of gas-phase Ir_5 is an edge-bridged square, with the bridging atom lifting out of the square-plane. The supported structure is a square-based pyramid structure with the basal plane lying parallel to the surface, forming four Ir-O bonds.

The supported and gas-phase structures of Au_4Ir are both tetrahedral structures. The supported structure is similar to that of supported Au_5 but the structure is now inverted and a single Ir-O bond is formed. The supported Au_3Ir_2, Au_2Ir_3 and $AuIr_4$ structures are all edge-bridged squares. The differences between these supported clusters and the corresponding gas-phase global minima vary. For Au_3Ir_2 the difference is simply a homotop swap maximising Ir-O bonds, whereas for Au_2Ir_3 there is a larger structural difference, with

a tetrahedral structure being preferred in the gas-phase.

AuIr$_4$ is found to have the same surface and the gas-phase structures; however the supported structure now only forms two Ir-O bonds, compared to the four Ir-O bonds of Ir$_5$. This may be due to an unfavourable interaction between the edge-bridging Au atom and the MgO(100) slab, had the Ir square remained four-coordinate, but it should be noted that the Ir4 square cluster also sits perpendicular to the surface, so it may just reflect the competition between the metal-on-top effect and localised Ir-O bonding effects.

The gas-phase structure of Ir$_6$ is a slightly bent double-square structure, with a 154° angle between squares. On the MgO(100)-support the structure is a 3D trigonal prism bound to the surface by four Ir-O bonds. The planar-triangular structure of Au$_6$ is found in both the gas-phase and on the surface. Au$_4$Ir and Au$_5$Ir have similar gas-phase and supported structures, with the extra Au in Au$_5$Ir capping a Au-Ir bond in the tetrahedral structure. On the surface, the structure of Au$_5$Ir is still based on the tetrahedral structure but the Au atom now caps a face.

Both Au$_4$Ir$_2$ and Au$_3$Ir$_3$ have the same planar-triangular structure on the surface and in the gas-phase. There are, however, differences in the homotop of each structure as they try to maximise Ir-O bonding. The Ir atoms in each surface-supported structure sit at the bottom of the structure, forming a dimer and trimer, for Au$_4$Ir$_2$ and Au$_3$Ir$_3$, respectively. Au$_2$Ir$_4$ has a planar bi-edge-bridged square structure in both the gas-phase and the surface, with the two bridging Au atoms adopting *cis* positions in the gas-phase GM and *trans* positions in the GM of the supported cluster. The gas-phase structure of AuIr$_5$ is similar to that of Au$_2$Ir$_4$ except that the bridging Ir sits out of plane of the square. The lowest energy AuIr$_5$ structure on the MgO(100) surface is an Ir$_5$ square pyramid (as for the Ir$_5$ cluster) with one of the edges on the square face bridged by Au. In contrast to Ir5, however, the square pyramid lies on its side on the MgO surface (with only 3 Ir atoms in contact with the surface) which may be due to an unfavourable interaction of the Au atom with the surface if the cluster sits with the square face on the surface.
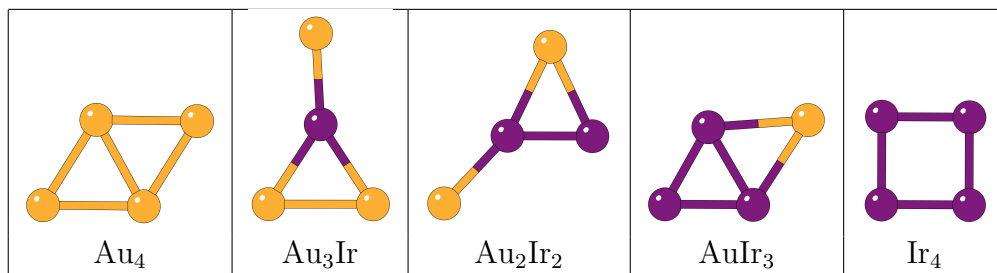
Figure 2: Putative global minimum structures of gas-phase Au_nIr_{4-n} clusters. Au and Ir are shown in gold and purple, respectively.
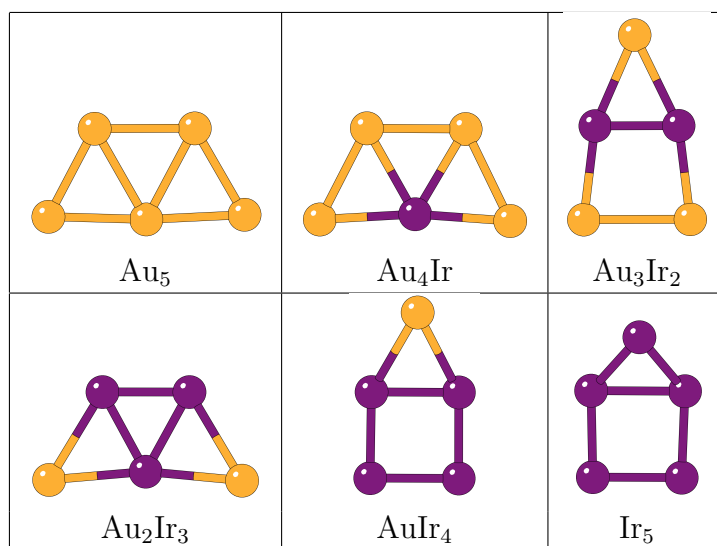

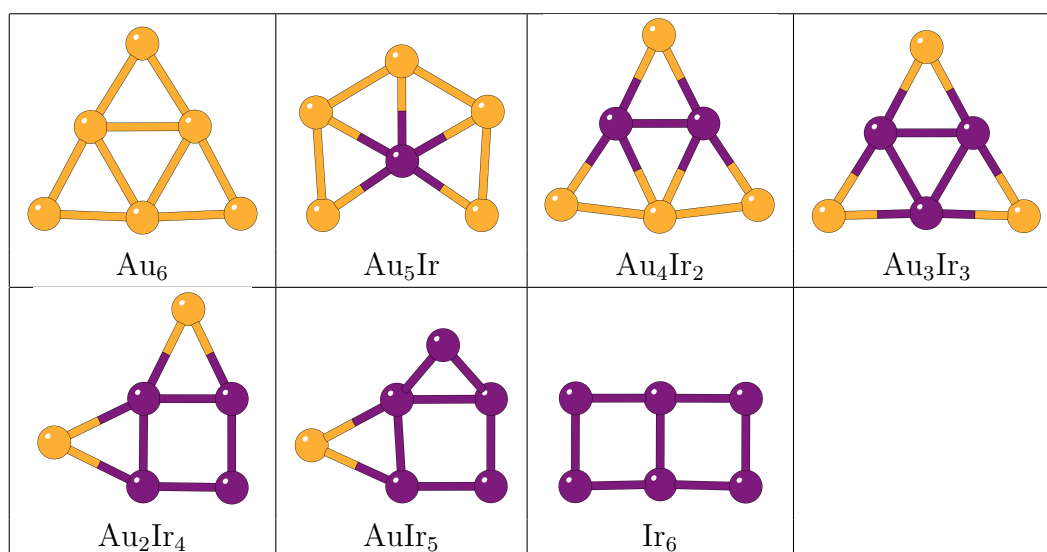Figure 3: Putative global minimum structures of gas-phase Au_nIr_{4-n} clusters.

Figure 4: Putative global minimum structures of gas-phase Au_nIr_{6-n} clusters.
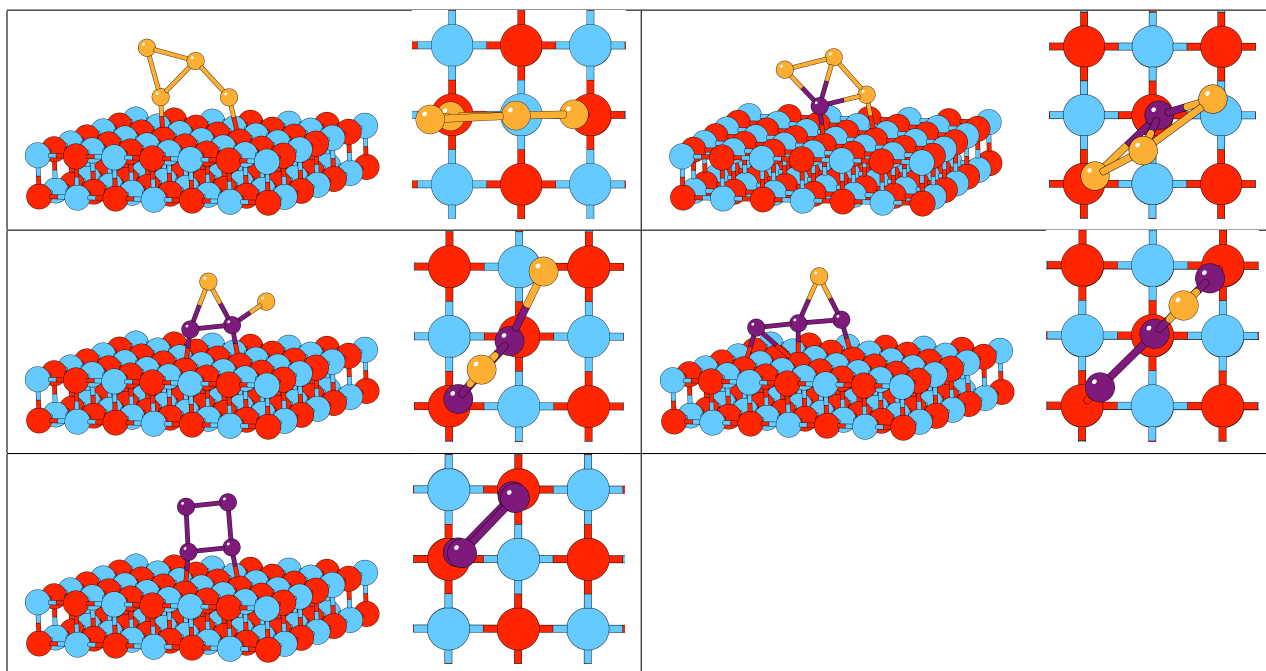
Figure 5: Putative global minimum structures of MgO(100)-supported Au_nIr_{4-n} clusters. Au, Ir, Mg and O are shown in gold, purple, red and blue, respectively.
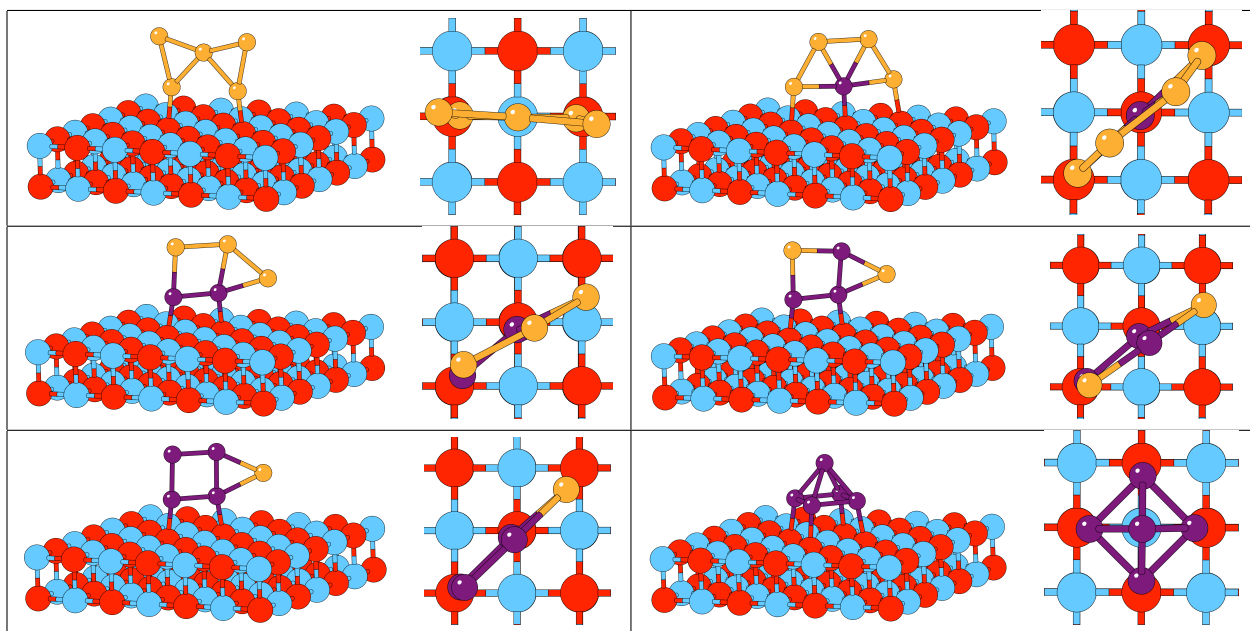

Figure 6: Putative global minimum structures of MgO(100)-supported Au_nIr_{5-n} clusters.
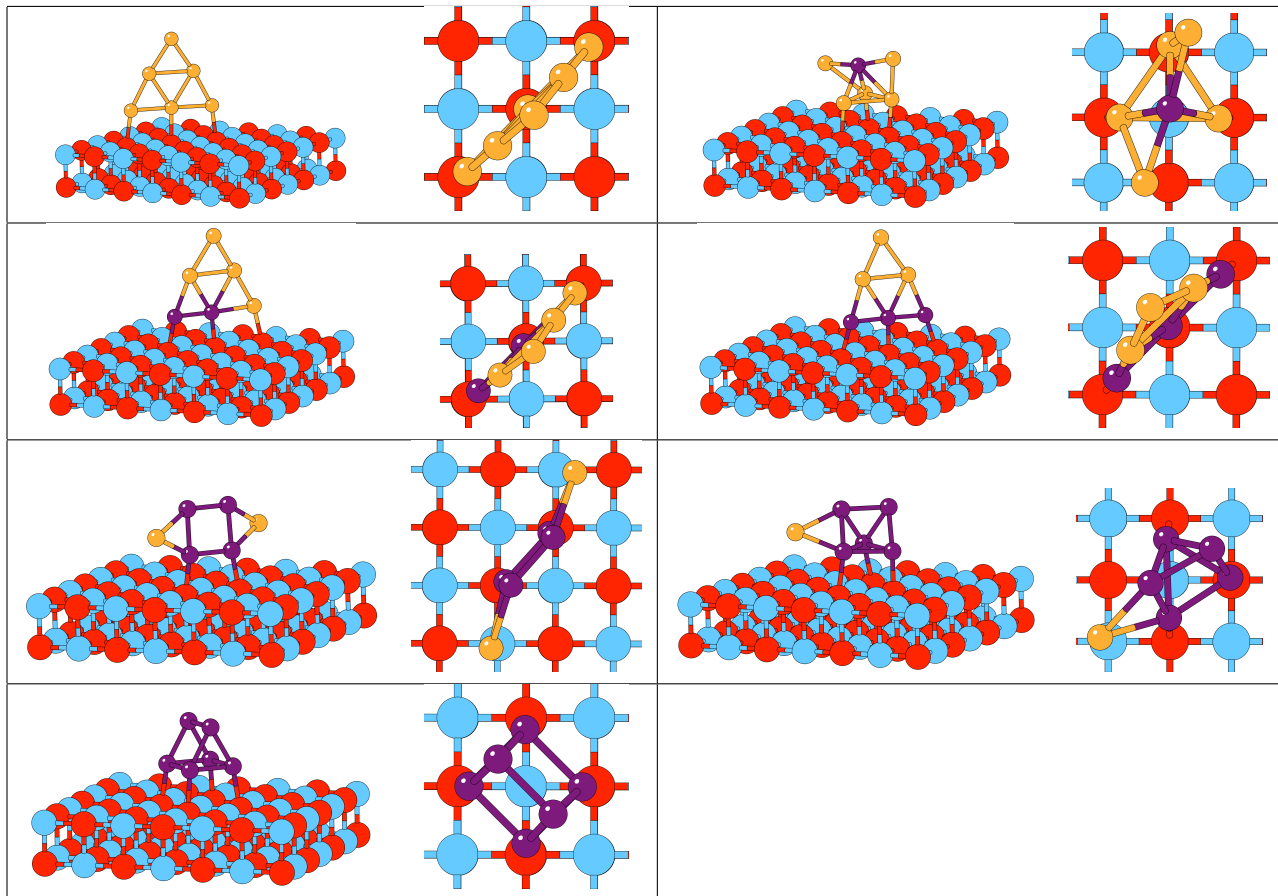
Figure 7: Putative global minimum structures of MgO(100)-supported Au_nIr_{6-n} clusters.

The results from our global optimisations, which are performed directly in the presence of an MgO(100) slab, can be compared with those from other studies, in which structures are generated in the gas-phase and are then deposited on a surface slab. Our results for Au compare favourably with structures found in both the gas-phase and on the surface.[33,34] However, work done previously on Ir clusters, using similar DFT calculations, which were generated in the gas-phase and deposited on the surface show clear differences for Ir_4 and Ir_6. This demonstrates the advantage of our methodology as the structures generated in the gas-phase greatly biases the structures found on the surface.

Work on surface-supported Ir is limited but results for Ir_4 and Ir_6 clearly differ from those reported in a recent study because of their utilisation of this methodology in their study.[35]

The spin multiplicities of the gas-phase and supported clusters are listed in table 1 and are plotted in figure 8. The Ir and Ir-rich clusters are generally found to possess higher spins than the Au and Au-rich clusters. The presence of the MgO(100) surface partially quenches the spins of the Ir and Au-Ir supported clusters, with the clusters processing lower-spin configurations. This is may be in part due to the Ir-O interactions which are favoured in these clusters, resulting in some of the unpaired Ir electrons being involved in Ir-O bonding. The surface is shown to have no overall effect on the spin of the Au clusters, which concurs with work done previously on Au.[33,34]

The adsorption energies E_{ads} of the supported clusters are listed in table 1 and are plotted in figure 9. There are differences between energies of supported clusters and the energies of the supported clusters with the slab removed, in particular the Au and Au-rich clusters are found to have the most negative E_{ads}, which then increases until the composition reaches around 50/50.

The excess energies plotted in figure 10, reveal the energetic preference for the alloy-ing of the constituent elements in the nanoalloy. AuIr is found to be a strongly demixing system, with positive Δ values found for almost all gas-phase and supported clusters sizes and compositions. The only negative values are found for $AuIr_4$, where from Ir_5 there is
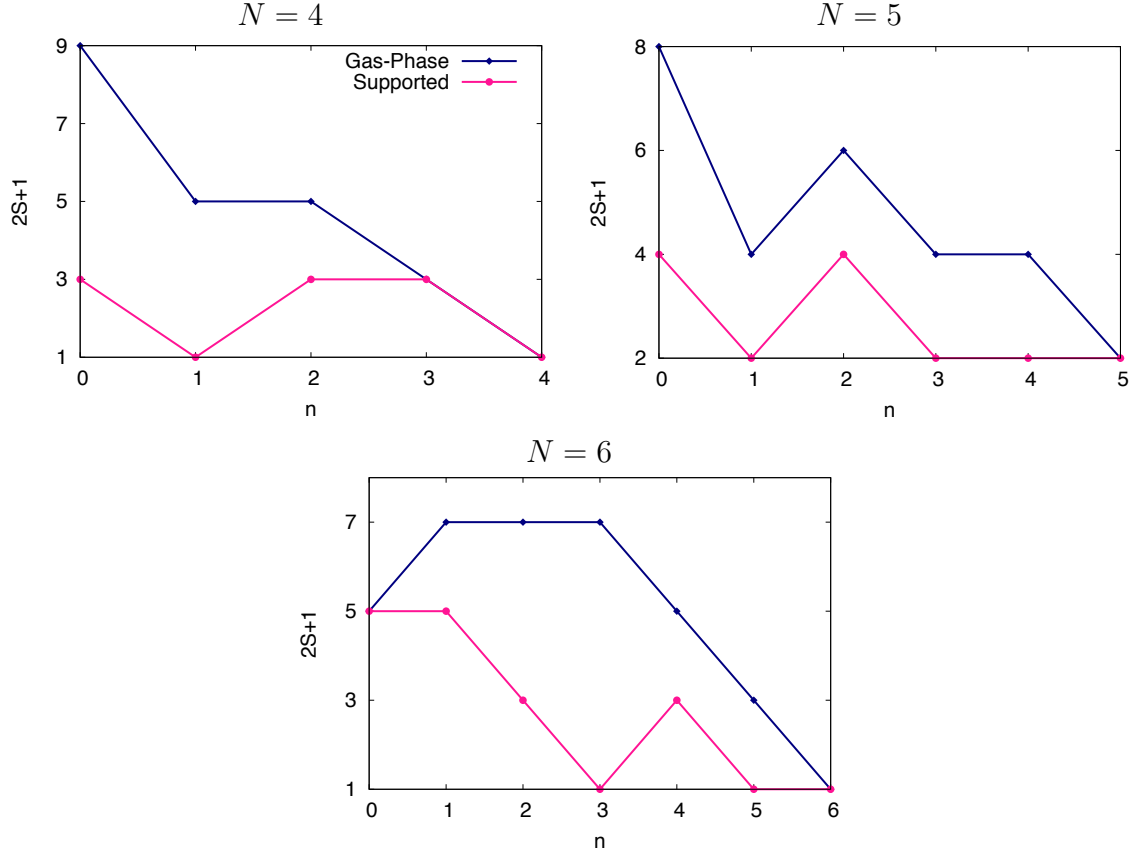
Figure 8: Spin multiplicities $2S + 1$ of the $N = 4 - 6$ Au_nIr_{N-n} gas-phase and MgO(100)-supported putative global minimum structures.

a 3D to 2D transition. The excess energies for the surface-supported clusters, particularly for 4 and 5-atoms, are found to have lower excess energies. In these cases the surface could be acting to promote alloying in the system. This trend, however, is not continued for the 6-atom clusters, with the gas-phase structures sometimes being less positive than those that are surface-supported.

Conclusions and Future Work

The BPGA has been successfully applied to the global optimisation of both gas-phase and MgO(100)-supported $N = 4 - 6$ Au_nIr_{N-n} clusters. The direct global optimisation in the presence of an MgO slab has revealed significant differences in gas-phase and surface-
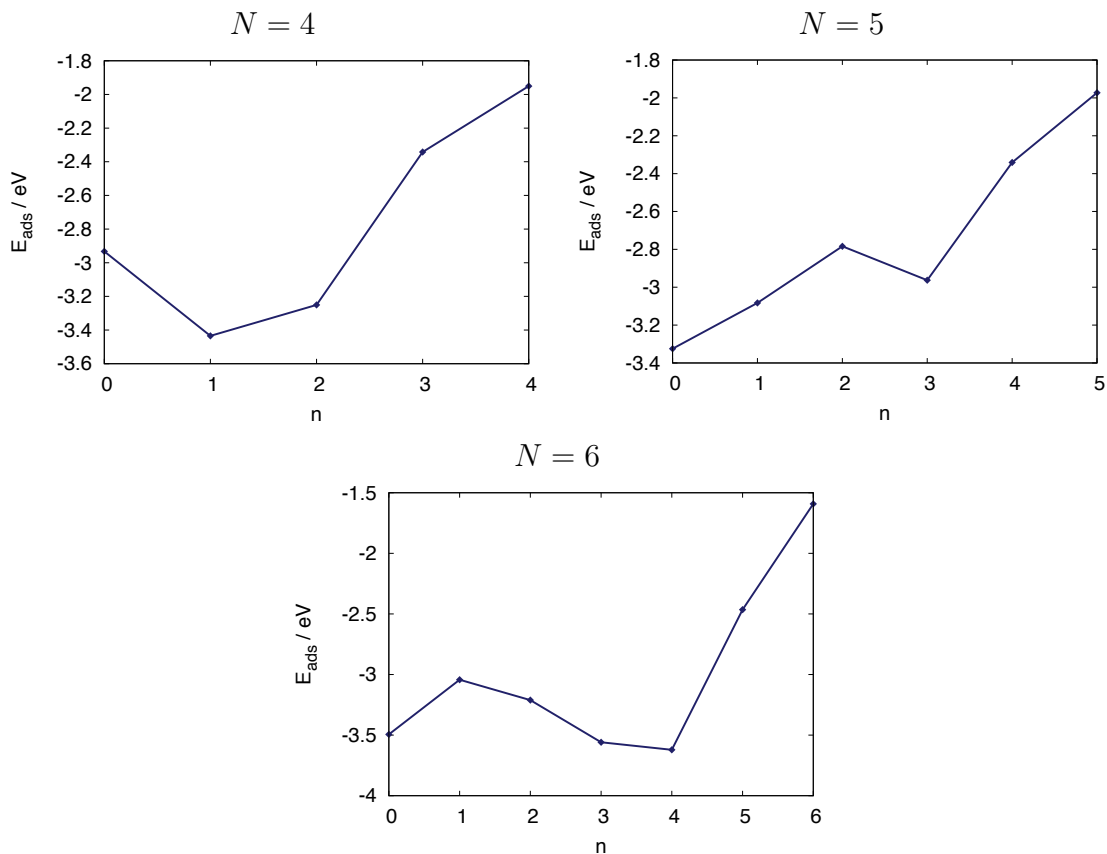
Figure 9: Adsorption energies E_{ads} of the MgO(100)-supported $N = 4-6$ $\mathrm{Au}_n\mathrm{Ir}_{N-n}$ clusters.

supported global minimum structures, with those on MgO(100) maximising the number of Ir-O bonds. The MgO(100) surface not only affects the structures and atomic ordering of the AuIr clusters, but the surface is also observed to suppress the spin of the clusters.

Future work will include expanding the BPGA's library of surface generators to include rutile, which has been shown to play an active role in increasing the catalytic performance of AuIr.[3] The larger number of surface sites on rutile will require greater computational effort and mutation schemes capable of exploring these sites completely during a search.

Acknowledgement

Figure 10: Excess energies E_Δ of the gas-phase and MgO(100)-supported $N = 4-6$ Au_nIr_{N-n} clusters.

References

(1) Johnston, R. L. *Atomic and Molecular Clusters*; Taylor and Francis: London, 2002.

(2) Ferrando, R.; Jellinek, J.; Johnston, R. L. Nanoalloys: From Theory to Applications of Alloy Clusters and Nanoparticles. *Chem. Rev.* **2008**, *108*, 845–910.

(3) Bokhimi, X.; Zanella, R.; Angeles-Chavez, C. Rutile-supported Ir, Au, and Ir-Au catalysts for CO oxidation. *J. Phys. Chem. C* **2010**, *114*, 14101–14109.

(4) Jiménez-Díaz, L. M.; Pérez, L. A. Structural and Electronic Properties of AuIr Nanoalloys. *Eur. Phys. J. D* **2013**, *67*, 15.

(5) Gómez-Cortés, A.; Díaz, G.; Zanella, R.; Ramírez, H.; Santiago, P.; Saniger, J. M. Au-Ir/TiO$_2$ Prepared by Deposition Precipitation with Urea: Improved Activity and Stability in CO Oxidation. *J. Phys. Chem. C* **2009**, *113*, 9710–9720.

(6) Aguilar-Tapia, A.; Zanella, R.; Calers, C.; Louis, C.; Delannoy, L. Synergistic effects of Ir Au / TiO 2 catalysts in the total oxidation of propene : influence of the activation conditions. *Phys. Chem. Chem. Phys.* **2015**, *17*, 28022–28032.

(7) Choudhary, T. V.; Goodman, D. W. Methane Activation on Ruthenium: The Nature of the Surface Intermediates. *Top. Catal.* **2002**, *20*, 35–42.

(8) Schubert, M. M.; Hackenberg, S.; van Veen, A. C.; Muhler, M.; Plzak, V.; Behm, R. J. CO Oxidation over Supported Gold CatalystsInert and Active Support Materials and Their Role for the Oxygen Supply during Reaction. *J. Catal.* **2001**, *197*, 113–122.

(9) Okumura, M.; Akita, T.; Haruta, M.; Wang, X.; Kajikawa, O.; Okada, O. Multi-Component Noble Metal Catalysts Prepared by Sequential Deposition Precipitation for Low Temperature Decomposition of Dioxin. *Appl. Catal. B* **2003**, *41*, 43–52.

(10) Heiles, S.; Johnston, R. L. Global Optimization of Clusters using Electronic Structure Methods. *Int. J. Quantum Chem.* **2013**, *113*, 2091–2109.

(11) Davis, J. B. A.; Shayeghi, A.; Horswell, S. L.; Johnston, R. L. The Birmingham Parallel

Genetic algorithm and its Application to the Direct DFT Global Optimisation of Ir$_N$ (N = 10-20) Clusters. *Nanoscale* **2015**, *7*, 14032–14038.

(12) Bandow, B.; Hartke, B. Larger Water Clusters with Edges and Corners on their way to Ice: Structural Trends Elucidated with an Improved Parallel Evolutionary Algorithm. *J. Phys. Chem. A* **2006**, *110*, 5809–5822.

(13) Vilhelmsen, L. B.; Hammer, B. A Genetic Algorithm for First Principles Global Structure Optimization of Supported Nano Structures. *J. Chem. Phys.* **2014**, *141*, 044711.

(14) Heard, C. J.; Heiles, S.; Vajda, S.; Johnston, R. L. Pd$_n$Ag$_{(4-n)}$ and Pd$_n$Pt$_{(4-n)}$ clusters on MgO (100): a density functional surface genetic algorithm investigation. *Nanoscale* **2014**, *6*, 11777–11788.

(15) Kresse, G.; Hafner, J. Ab Initio Molecular Dynamics for Liquid Metals. *Phys. Rev. B* **1993**, *47*, 558–561.

(16) Kresse, G.; Hafner, J. Ab Initio Molecular-Dynamics Simulation of the Liquid-Metal-Amorphous-Semiconductor Transition in Germanium. *Phys. Rev. B* **1994**, *49*, 14251–14269.

(17) Kresse, G.; Furthmüller, J. Efficiency of Ab-Initio Total Energy Calculations for Metals and Semiconductors using a Plane-Wave Basis Set. *Comput. Mater. Sci.* **1996**, *6*, 15–50.

(18) Kresse, G.; Furthmüller, J. Efficient iterative schemes for ab initio total-energy calculations using a plane-wave basis set. *Physical Review. B* **1996**, *54*, 11169–11186.

(19) Monkhorst, H. J.; Pack, J. D. Special points for Brillouin-zone integrations. *Phys. Rev. B* **1976**, *13*, 5188–5192.

(20) Perdew, J.; Burke, K.; Wang, Y. Generalized Gradient approximation for the Exchange-Correlation Hole of a Many-Electron System. *Phys. Rev. B* **1996**, *54*, 533–539.

(21) Kresse, G.; Joubert, D. From Ultrasoft Pseudopotentials to the Projector Augmented-Wave Method. *Phys. Rev. B* **1999**, *59*, 1758 – 1775.

(22) Methfessel, M.; Paxton, A. T. High-precision Sampling for Brillouin-Zone Integration in Metals. *Phys. Rev. B* **1989**, *40*, 3616–3621.

(23) https://bitbucket.org/JBADavis/bpga/.

(24) Shayeghi, A.; Götz, D.; Davis, J. B. A.; Schäfer, R.; Johnston, R. L. Pool-BCGA: a Parallelised Generation-Free Genetic Algorithm for the Ab Initio Global Optimisation of Nanoalloy Clusters. *Phys. Chem. Chem. Phys.* **2015**, *17*, 2104–2112.

(25) Deaven, D. M.; Ho, K. M. Molecular Geometry Optimization with a Genetic Algorithm. *Phys. Rev. Lett.* **1995**, *75*, 288–291.

(26) Gro, H.; Broqvist, P. CO-Induced Modification of the Metal/MgO(100) Interaction. *J. Phys. Chem. B* **2003**, *107*, 12239–12243.

(27) Grönbeck, H.; Broqvist, P. Pt and Pt_2 on MgO(100) and BaO(100): Structure, Bonding, and Chemical Properties. *J. Chem. Phys.* **2003**, *119*, 3896–3904.

(28) Ferrando, R.; Fortunelli, A. Diffusion of Adatoms and Small Clusters on Magnesium Oxide Surfaces. *J. Phys.: Condens. Matter* **2009**, *21*, 264001.

(29) Ismail, R.; Ferrando, R.; Johnston, R. L. Theoretical Study of the Structures and Chemical Ordering of Palladium-Gold Nanoalloys Supported on MgO(100). *J. Phys. Chem. C* **2013**, *117*, 293–301.

(30) Ferrando, R.; Fortunelli, A.; Rossi, G. Quantum effects on the structure of pure and binary metallic nanoclusters. *Phys. Rev. B* **2005**, *72*, 085449.

(31) Barcaro, G.; Fortunelli, A. The Interaction of Coinage Metal Clusters with the MgO(100) Surface. *J. Chem. Theory Comput.* **2005**, *1*, 972–985.

(32) Pawluk, T.; Hirata, Y.; Wang, L. Studies of Iridium Nanoparticles Using Density Functional Theory Calculations. *J. Phys. Chem. B* **2005**, *109*, 20817–20823.

(33) Frondelius, P.; Hakkinen, H.; Honkala, K. Adsorption of small Au clusters on MgO and MgO/Mo: the role of oxygen vacancies and the Mo-support. *N. J. Phys.* **2007**, *9*, 339.

(34) Frondelius, P.; Häkkinen, H.; Honkala, K. Adsorption of gold clusters on metal-supported MgO : Correlation to electron affinity of gold. *Phys. Rev. B* **2007**, *76*, 073406.

(35) Chen, Y.; Huo, M.; Chen, T.; Li, Q.; Sun, Z.; Song, L. The Properties of Ir_n (n = 2-10) Clusters and their Nucleation on γ-Al_2O_3 and MgO Surfaces: from Ab Initio Studies. *Phys. Chem. Chem. Phys.* **2015**, *17*, 1680–1687.

Graphical TOC Entry